J Mater Sci: Mater Med (2011) 22:1221–1230
DOI 10.1007/s10856-011-4304-9

A fibrin gel loaded with chitosan nanoparticles for local delivery of rhEGF: preparation and in vitro release studies

Wenjun Zhou · Min Zhao · Yuan Zhao · Yan Mou

Received: 1 December 2010 / Accepted: 21 March 2011 / Published online: 29 March 2011

Abstract Recombinant human epidermal growth factor (rhEGF) is known to stimulate cell proliferation and accelerate wound healing. Direct delivery of rhEGF at the wound site in a sustained and controllable way without loss of bioactivity would enhance its biological effects. The aim of this study was to prepare a novel local delivery system for the sustained and controllable release of rhEGF, a fibrin gel loaded with chitosan nanoparticles. First, rhEGF-loaded chitosan nanoparticles were prepared and characterized, and these showed an ability to protect rhEGF from proteolysis. The prepared nanoparticles were then incorporated into a fibrin gel matrix during polymerization. In vitro release studies showed that the fibrin gel loaded with rhEGF/chitosan nanoparticles could achieve a more sustained release of rhEGF than either chitosan nanoparticles or an unloaded fibrin gel. Additionally, the release rate could be controlled by altering the contents of fibrinogen and thrombin in this composite delivery system. The bioactivity of the released rhEGF was determined by assessing its ability to stimulate the proliferation of BALB/c 3T3 cells, and the results showed that rhEGF bioactivity was not affected during the preparation process and could be maintained for at least 7 days. This novel delivery system may have great potential applications in the local administration of rhEGF.

W. Zhou · M. Zhao (✉) · Y. Zhao · Y. Mou
Chongqing Key Laboratory of Ophthalmology, Chongqing Eye Institute, The First Affiliated Hospital of Chongqing Medical University, No. 1, Youyi Road, Yu Zhong District, Chongqing 400016, China
e-mail: cqminzhao@163.com

1 Introduction

Epithelial growth factor (EGF) is a single-chain polypeptide containing 53 amino acid residues (MW = 6,045) and three disulfide bridges that are required for biological activity [1]. The polypeptide stimulates the proliferation of epidermal cells and other types of cells such as fibroblasts and endothelial cells [2]. Moreover, EGF also inhibits gastric acid secretion and accelerates wound healing [3, 4]. Based on its wound-healing properties, EGF is an attractive candidate for a therapeutic drug. Many studies have investigated the application of EGF for the treatment of wounds. However, due to its susceptibility to proteolysis and denaturation [5], a relatively short half life [6], the loss of occupied receptors through turnover and a lag time of 8–12 h to commit cells to DNA synthesis [7], maintaining an effective topical concentration at the wound site for a certain period time has become vital in the application of EGF. Therefore, the development of a suitable delivery system for EGF to achieve a sustained release and improve its bioavailability is necessary.

In recent years, polymer nanoparticles have attracted considerable attention as potential drug-delivery vehicles. Chitosan (CS), a linear cationic polysaccharide composed of deacetylated beta-1,4-D-glucosamine, has been considered as a candidate pharmaceutical material because it is biocompatible, biodegradable and nontoxic [8]. The formation of chitosan into nanoparticles has been proven to be a promising method for the delivery of peptides, proteins, oligonucleotides, and plasmids [9, 10]. In vitro studies have showed that CS nanoparticles can achieve a sustained release of drugs and have the ability to protect sensitive bioactive materials from enzymatic and chemical degradation [11, 12]. However, encapsulated drugs tend to be released in an uncontrolled manner and often show a burst-release profile in the initial phase.

Fibrin gel, a network formed when fibrinogen is activated by thrombin in the presence of Ca^{2+} ion and Factor XIII, has been reported as another potential drug-delivery system. Fibrin gel with an incorporated drug can be easily injected, forming a drug reservoir for local delivery at the desired site. In previous studies, fibrin gel has been used as a matrix to deliver growth factors, including nerve growth factor [13], basic fibroblast growth factor (bFGF) [14], vascular endothelial growth factor (VEGF) [15], transforming growth-factor beta [16] and rhEGF [17]. Moreover, it has been demonstrated that the release rate of bFGF or VEGF can be controlled by altering the concentrations of thrombin and fibrinogen [18]. However, even when rhEGF is administrated in a gel formulation, it is expected that there would be poor bioavailability of rhEGF in the wound due to the instability of the protein [19].

In the present study, we prepared a novel delivery system by combining CS nanoparticles and a fibrin gel to create an efficient vehicle for rhEGF delivery. First, rhEGF-loaded CS nanoparticles were prepared and characterized, and the stability of the rhEGF encapsulated in the nanoparticles was examined. The rhEGF/CS nanoparticles were then incorporated into a fibrin gel and the effects of altering fibrinogen and thrombin concentrations on the release of rhEGF from this composite fibrin gel were investigated. Finally, the bioactivity of the released rhEGF was evaluated by stimulating proliferation of mouse embryonic fibroblasts (BALB/c 3T3). Based on the results, we concluded that this new delivery system can release rhEGF in a sustained and controllable way. When administrated locally, the fibrin gel can act as a drug reservoir and the CS nanoparticles should improve rhEGF stability in the wound site.

2 Materials and methods

2.1 Materials

Chitosan in the form of a hydrochloride salt (MW: <150 kD, deacetylation degree: >80%) was purchased from Sangon Biotech Co. (Shanghai, China). Pentasodium tripolyphosphate (TPP) was purchased from Sinopharm Chemical Reagent Co. (Shanghai, China). rhEGF and an rhEGF ELISA kit were purchased from R&D Systems Co. (USA). Commercially available fibrin gel kits were purchased from Beixiu Biotech Co. (Guangzhou, China). New Zealand rabbits were obtained from the animal center at Chongqing Medical University (Chongqing, China). Balb/3T3 cells were obtained from the cell bank of the Chinese Academy of Science (Shanghai, China). All the materials used in the cell-culture study, including Dulbecco's Modified Eagles' Medium (DMEM), heat-inactivated fetal bovine serum (FBS), trypsin from porcine pancreas and 3-(4,5-dimethylthiazol-2-yl)-2,5-diphenyl tetrazolium bromide (MTT), were obtained from Sigma-Aldrich Chemical Co. (USA). All other chemicals were of analytical grade.

2.2 Preparation of rhEGF-loaded chitosan nanoparticles

Chitosan nanoparticles were prepared according to the ionotropic gelation process. Blank nanoparticles were obtained upon the addition of an aqueous TPP solution (0.5 mg/ml) to a CS solution (1.0 mg/ml) stirred at room temperature. Various volume ratios of CS/TPP (1:3, 1:2, 1:1, 2:1, 3:1, 4:1, 5:1, 6:1) were investigated during the formation in order to minimize the size of CS nanoparticles. Three kinds of phenomena were observed: solution, aggregates and opalescent suspension. The zone of opalescent suspension was further examined as nanoparticles, and the formulation with the CS/TPP ratio of 3:1 was found to have the minimum particle size. The rhEGF-loaded nanoparticles were obtained according to the same procedure. Various concentrations of rhEGF were added to the chitosan solution prior to the formation of nanoparticles to investigate the effect of the initial peptide concentration on the nanoparticle characteristics. The formation of nanoparticles was a result of the interaction between the negative groups of TPP and the positively-charged amino groups of chitosan. For further study, the nanoparticles were collected by centrifugation at 10,000 rpm and 4°C on a 10 μl glycerol bed for 1 h (Sigma 3K15, Germany) and the supernatants were discarded.

2.3 Physicochemical characterization of rhEGF-loaded chitosan nanoparticles

The mean size, size distribution (polydispersity index) and zeta potential of the nanoparticles were determined by photon-correlation spectroscopy and laser Doppler anemometry, respectively, in triplicate using a Zetasizer Nano ZS90 (Malvern Instrument, UK).

The morphological examination of the chitosan nanoparticles was performed using a transmission electron microscope (TEM; Tecnai-10, Philip, Japan). Samples of the nanoparticle suspension (5–10 μl) were dropped onto a carbon-film-coated 200 mesh copper grid and allowed to air dry for 10 min. The samples were stained with 1% (w/v) aqueous uranyl acetate solution for 1.5 min and any excess uranyl acetate was removed with filter paper before viewing on the TEM.

The morphology of the nanoparticles was also examined by scanning electron microscopy (SEM). Liquid samples were deposited on a carbon-film-coated 200 mesh copper grid and air dried at room temperature. The samples were

sputter-coated with gold before being examined on a scanning electron microscope (S-3400 N, Hitachi, Japan).

2.4 Evaluation of rhEGF encapsulation

The rhEGF/CS nanoparticles were separated from the aqueous suspension medium by ultracentrifugation at 10,000 rpm and 4°C for 1 h. The amount of free rhEGF in the clear supernatant was determined with an enzyme-linked immunosorption assay (ELISA) kit. Briefly, standards and samples were pipetted into the antibody-coated 96-well microtiter plate and incubated at 37°C for 2 h. Any rhEGF present would be bound by the immobilized antibody. After washing, a horseradish-peroxidase-conjugated polyclonal antibody against rhEGF was added and the plates were incubated at 37°C for 1 h. After a washing step, the substrate (tetramethylbenzidine) solution was added which reacted with the bound enzyme to produce a color change. The reaction was stopped by acidification, and rhEGF was quantified by measuring the absorption at 450 nm in the reader (SpectraMax M2 microplate reader, Molecular Devices, USA). The encapsulation efficiency (EE) of the chitosan nanoparticles were calculated according to the following equation: %EE = 100 × [(total rhEGF−free rhEGF)/total rhEGF]. All measurements were performed in triplicate.

2.5 Stability of rhEGF in mucosal homogenates

New Zealand rabbits were euthanized by air embolism after being deeply anesthetized by intravenous administration of an overdose of pentobarbital sodium (3%). The rabbit conjunctivae were then removed by cutting at the base, rinsed in chilled isotonic saline, and placed in borosilicate glass vials. The collected mucosal tissue was immediately homogenized in an isotonic phosphate buffer cooled with an ice bag. The homogenates were centrifuged at 3,000×*g* and 4°C for 15 min and the supernatant was collected. To assess the stability of rhEGF against proteolytic degradation, free rhEGF and chitosan nanoparticles (Group V, Table 1) containing equal amounts of rhEGF (both 100 μg) were mixed separately with the supernatant (1 ml). The amount of rhEGF in the nanoparticles was calculated according to the encapsulation efficiency (EE). The mixture was incubated for 6 h at 37°C in a shaking water bath. Subsequently, the incubation mixture was sampled at predetermined time intervals. The reaction was stopped by the addition of acetonitrile and vortexed for 10 s. After centrifugation for 10 min at 10,000×*g*, the supernatant was evaporated under a stream of nitrogen. The residues were redissolved with 100 μl of the mobile phase for HPLC analysis, a mixture of acetonitrile, triethylamine and water (pH 6.5) in a 250:2.2:850 (v/v/v) ratio. Separation was achieved on a Vydac® protein and peptide C_{18} column. The flow rate was 0.8 ml/min and detection was monitored at 214 nm.

The experimental procedures complied with the University Animal Ethics Committee Guidelines. The study was approved by the University Animal Ethics Committee.

2.6 Incorporation of nanoparticles into fibrin glue

The fibrin glue kit consisted of fibrinogen and thrombin from bovine plasma in separate vials, plus separate solutions of potassium dihydrogen phosphate (KDP) and calcium chloride ($CaCl_2$). The rhEGF/CS-nanoparticle-incorporated fibrin gel was prepared as follows. The fibrinogen, containing Factor XIII and approximately 60 U/100 mg fibrinogen, was reconstituted in the KDP solution and then drawn into a syringe. Thrombin was reconstituted in a 40 mM $CaCl_2$ solution and then rhEGF/CS nanoparticles (Group V, Table 1) were added to this solution before being taken up into another syringe. Both the syringes were loaded into the syringe holder of the fibrin-glue-delivery system. Using a common plunger, both components were pushed through separate channels into a common needle head and delivered out to form a fibrin clot. To examine the morphology, the clot was delivered onto a piece of cover slip (8 mm × 8 mm) and clot formation was allowed to continue for 1 h at 20°C. The clot was then incubated in 4% glutaraldehyde in phosphate-buffered saline solution (PBS) for 3 h at 4°C and dehydrated by passage through a graded series of ethanol and tertiary butyl alcohol (50, 70, 80, 90, and 100%) for 10 min at each concentration. After air drying, the sample was sputter-coated with gold before being examined on a scanning electron microscope (S-3400 N, Hitachi, Japan).

2.7 In vitro kinetics of rhEGF release

rhEGF release from CS nanoparticles (Group V, Table 1) was determined as follows: precipitated nanoparticles were resuspended in 1 ml of PBS and incubated at 37°C under light agitation. At intervals of 12 h, individual samples were centrifuged and the amount of the peptide in the release medium was determined using an ELISA kit.

To determine rhEGF release kinetics from nanoparticle-incorporated fibrin clots, samples (500 μl) with various concentrations of fibrinogen and thrombin containing either free rhEGF or rhEGF/CS nanoparticles (Table 2) were polymerized in 2 ml microcentrifuge tubes containing 1 ml of PBS (pH 7.4). The samples were incubated at 37°C under continuous agitation. The supernatant was withdrawn at various time points and the samples replenished with fresh buffer. The amounts of rhEGF in the supernatants were determined with an ELISA kit.

Table 1 Physicochemical properties of chitosan nanoparticles containing different concentrations of rhEGF ($n = 3$)

	Initial rhEGF (μg/ml)	Particle size (nm)	Zeta potential (mV)	P.I.	%EE
I	0	282.5 ± 5.0	43.7 ± 0.8	0.19 ± 0.02	–
II	1.0	268.2 ± 1.9	35.7 ± 0.4	0.19 ± 0.03	66.67 ± 2.08
III	1.5	276.3 ± 2.9	35.1 ± 0.4	0.21 ± 0.03	65.93 ± 2.14
IV	2.0	288.6 ± 2.8	34.2 ± 0.3	0.26 ± 0.02	64.13 ± 4.48
V	2.5	275.7 ± 6.8	32.7 ± 0.6	0.23 ± 0.04	67.03 ± 1.22
VI	3.0	264.0 ± 4.2	31.3 ± 0.5	0.22 ± 0.03	54.87 ± 2.94

2.8 rhEGF bioactivity assay

Mouse embryonic fibroblasts (BALB/c 3T3) were maintained in a basal medium (a 2:1 mixture of DMEM/F12 and PBS), supplemented with 10% (v/v) fetal bovine serum, 100 U/ml penicillin, 100 μg/ml streptomycin and 2 mM L-glutamine. The bioactivity of rhEGF released from the nanoparticle-incorporated fibrin clots (Group II, Table 2) was assessed in vitro by determining its ability to stimulate the proliferation of BALB/c 3T3 cells. Fibrin-clot samples were placed in 2 ml microcentrifuge tubes with 1 ml basal medium containing FBS and antibiotics. At 1, 3, 5 and 7 days, media were removed from the tubes and replaced with fresh media.

BALB/c 3T3 cells were seeded in 96-well plates at a density of 5×10^3 cells/well. After 24 h, the medium was replaced with the medium collected from the tubes. After an incubation time of 72 h, cell numbers were determined by a 3-(4,5-dimethylthiazol-2-yl)-2,5-diphenyl tetrazolium bromide (MTT) assay. As positive control, soluble rhEGF was added daily to the cell medium in amounts equivalent to those released from the fibrin clots. The amount of growth factor added daily was calculated from the release kinetics obtained from the in vitro release study described above. Cell culture in the basal medium without rhEGF served as a negative control.

Table 2 Fibrin gels containing rhEGF/CS nanoparticles or free rhEGF with various concentrations of fibrinogen and thrombin

	Fibrinogen (mg/ml)	Thrombin (U/ml)	rhEGF/CS nanoparticles[a] (μg)[b]	free rhEGF (μg)
Group I	50	50	2	0
Group II	50	100	2	0
Group III	50	200	2	0
Group IV	50	100	0	2
Group V	25	100	2	0
Group VI	100	100	2	0

[a] rhEGF/CS nanoparticles with a average %EE of 67.03% (Group V, Table 1)

[b] The amount of rhEGF in CS nanoparticles, calculated according to %EE

2.9 Statistical analysis

Statistical analyses were undertaken using Origin 8.0 software. Data were compared using a Student's t test, and a one-way ANOVA with a Bonferroni post-test was used for group analysis. The results are expressed as a mean and standard deviation (S.D.). Statistical significance was considered at a probability of $P < 0.05$.

3 Results

3.1 Physicochemical characterization and encapsulation of rhEGF/CS nanoparticles

Table 1 presents the physicochemical properties of CS nanoparticles prepared with various concentrations of initial rhEGF. The average particle size of the nanoparticles ranged from approximately 260–290 nm. As the initial rhEGF concentration was increased, the particle size did not become larger, as was expected. It appears that the amount of encapsulated rhEGF is too small to affect the size of the nanoparticles. Figure 1 shows TEM (a) and SEM (b) photographs of rhEGF/CS nanoparticles. The particles were spherical, distinct and regular. It is noteworthy that the hydrodynamic diameter of the particles measured by light scattering was higher than the size estimated by microscopy. This can be explained by the dehydration of the CS hydrogel nanoparticles during sample preparation for imaging. The CS nanoparticles had a positive zeta potential ranging from approximately 31–44 mV, varying with the rhEGF content. CS nanoparticles exhibited a high encapsulation efficiency of up to 60% in each group except group VI (54.87%, Table 1). The formulation with the initial peptide concentration of 2.5 μg/ml provided the highest encapsulation efficiency (67.03%). There was no apparent correlation between the rhEGF concentration and the encapsulation efficiency.

3.2 Stability of rhEGF in mucosal homogenates

To determine whether the encapsulation of rhEGF by CS nanoparticles could protect rhEGF against enzymatic degradation, conjunctival homogenates were prepared to simulate a wound environment. The degradation of rhEGF after incubation with the homogenates was determined by measuring the loss of rhEGF using HPLC analysis. As shown in Fig. 2, free rhEGF was rapidly degraded in the conjunctival homogenates; nearly 50% rhEGF was lost during the first hour and only 12% was left after 6 h. The nanoparticle-encapsulated rhEGF was much more stable, with 40% undegraded after 6 h. This observation indicates that CS nanoparticles can potentiate rhEGF activity and substantially prolong its biological half-life.

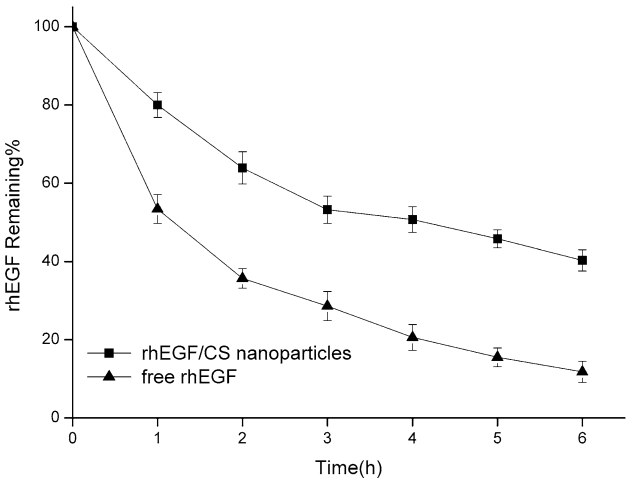

Fig. 2 Proteolysis profile of rhEGF in conjunctival homogenate of New Zealand rabbit. There was a significant difference between the proteolysis profiles of free rhEGF and rhEGF/nanoparticles at each time point ($n = 3$; mean ± S.D., $P < 0.05$, Student's t test)

3.3 Incorporation of nanoparticles into fibrin glue

The microstructures of the fibrin gels loaded with and without rhEGF/CS nanoparticles are displayed in Fig. 3a, b. The fibrin fiber thickness, density, and degree of branching and the size of the pores of the fibrin network appeared uninfluenced by the presence of the rhEGF/CS nanoparticles. No distinct structural differences could be observed between the two fibrin gels. The network was composed of tightly-woven fibrin fibers, and the CS nanoparticles seemed undamaged by the fibrin gel-formation process. As observed, they still maintained a spherical shape and were adsorbed at the surface of fibrin fibers.

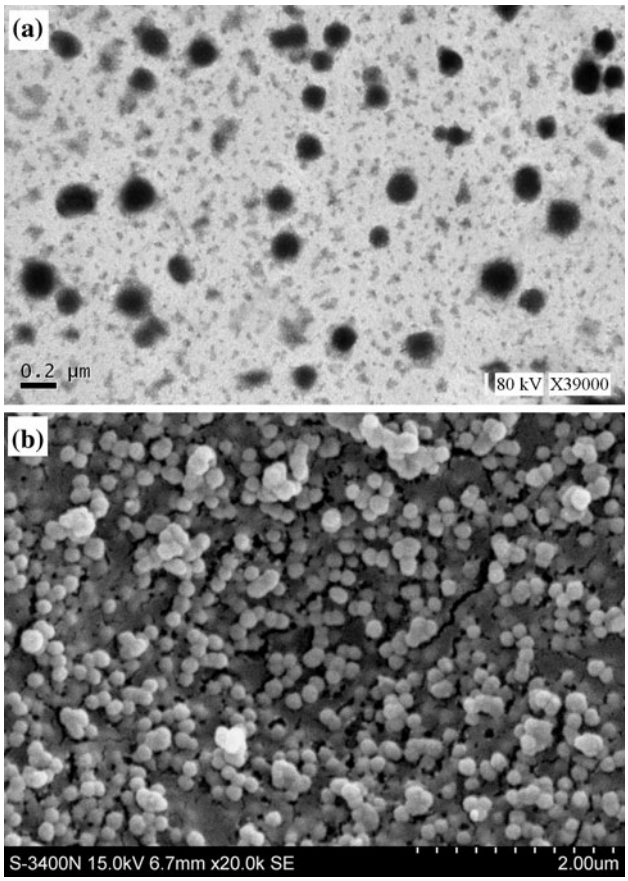

Fig. 1 TEM (**a**) and SEM (**b**) photographs of rhEGF/CS nanoparticles (chitosan 1.0 mg/ml, TPP 0.5 mg/ml, rhEGF 2.5 μg/ml)

3.4 In vitro kinetics of rhEGF release

Figure 4 shows the in vitro release kinetics of rhEGF from the CS nanoparticles, fibrin glue and nanoparticle-incorporated fibrin glue. When rhEGF was released from the CS nanoparticles, a burst release of approximately 65% of the rhEGF occurred within the first 12 h, followed by a slow release phase sustained for approximately 72 h. The burst release of rhEGF was not as obvious for fibrin glue; approximately 35% of the rhEGF was released within 12 h and 56% within 24 h. Compared with the two systems above, the nanoparticle-incorporated fibrin glue released rhEGF more gradually and more steadily. Approximately 35% of rhEGF was still not released from this system after 96 h. This indicates that the combination of CS nanoparticles and fibrin gel form a system with a more sustained release.

Furthermore, we investigated the effect of fibrinogen and thrombin concentrations on the rhEGF release kinetics from the composite fibrin glue. As shown in Figs. 5, 6, the rhFGF release rate decreased as the thrombin and the fibrinogen contents in the composite fibrin gels was increased. In Fig. 5, almost all of the rhEGF was released from the fibrin gels with low thrombin concentrations of 50 U/ml (Group I, Table 2) within 9 days. In contrast, 10%

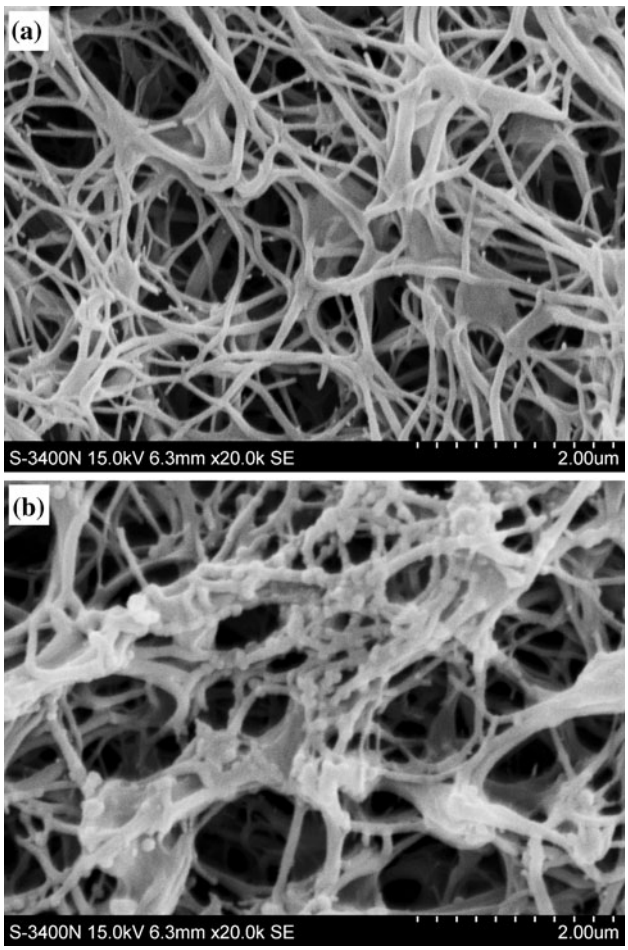

Fig. 3 SEM micrograph of fibrin networks in the presence and absence of rhEGF/CS nanoparticles (fibrin clot without nanoparticles (**a**), fibrin clot with nanoparticles (**b**), fibrinogen 50 mg/ml, thrombin 100 U/ml)

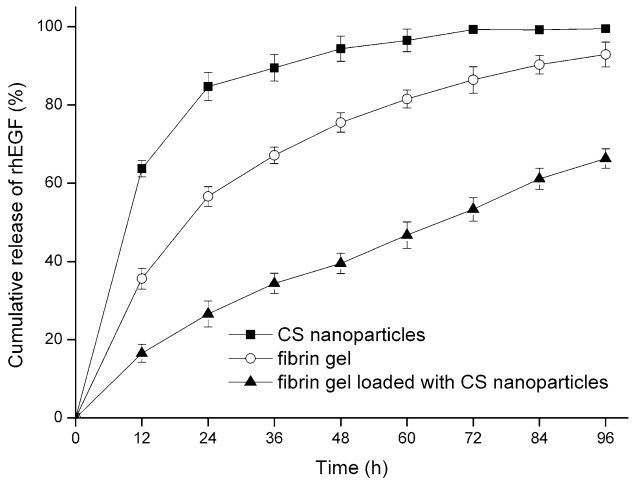

Fig. 4 Profile of rhEGF release from CS nanoparticles (Group V, Table 1), fibrin gel (Group IV, Table 2) and fibrin gel loaded with CS nanoparticles (Group II, Table 2). Cumulative release percentages of rhEGF from fibrin gel loaded with CS nanoparticles were significantly different at each time point compared with those from CS nanoparticles or fibrin gel, respectively ($n = 5$; mean ± S.D., $P < 0.05$, Student's t test)

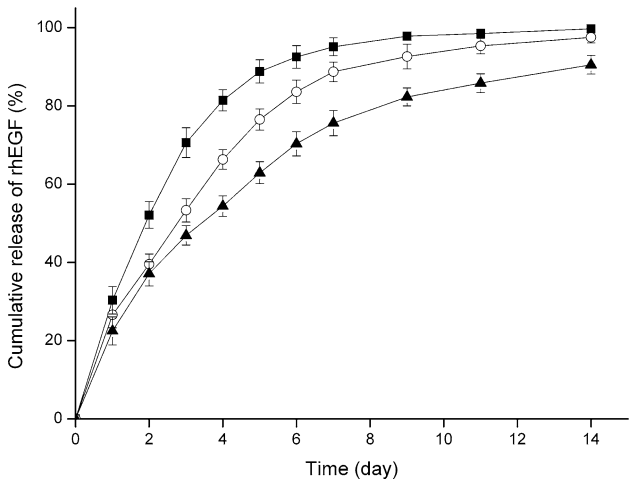

Fig. 5 Cumulative release of rhEGF from nanoparticle incorporated fibrin gels prepared at different thrombin concentrations [Table 2; Group I, thrombin, 50 U/ml (*filled square*); Group II, thrombin, 100 U/ml (*open circle*); Group III, thrombin, 200 U/ml (*filled triangle*)]. The values represent the mean ± S.D. ($n = 5$)

of the initially loaded rhEGF still remained after 14 days in the fibrin gels with a high thrombin concentrations of 200 U/ml (Group III, Table 2). In Fig. 6, almost all of the rhEGF was released from the fibrin gels with low fibrinogen concentrations of 25 mg/ml (Group V, Table 2) within 7 days. In contrast, 25% of the initially loaded rhEGF still remained after 14 days in the fibrin gels with a high fibrinogen concentrations of 100 mg/ml (Group VI, Table 2). At the median concentrations of both fibrinogen and thrombin, the rhEGF release sustained approximately for 14 days (Group II, Table 2).

3.5 rhEGF bioactivity assay

The in vitro proliferation of BALB/c 3T3 cells induced by rhEGF released from the composite fibrin gels (Group II, Table 2) was evaluated to test its biological activity. Proliferating cell numbers were determined by the MTT assay on BALB/c 3T3 cells incubated for 72 h with media collected from the composite gels at 1, 3, 5 and 7 days, or media containing known amounts of soluble rhEGF (positive control) and media containing no rhEGF (negative control). Compared with the negative control, cell numbers were significantly increased in the experimental group and positive control group at each time point. However, no significant difference in cell growth between the composite gel and positive control was revealed (Fig. 7). These results indicate that rhEGF released from the composite gel was bioactive for up to 7 days.

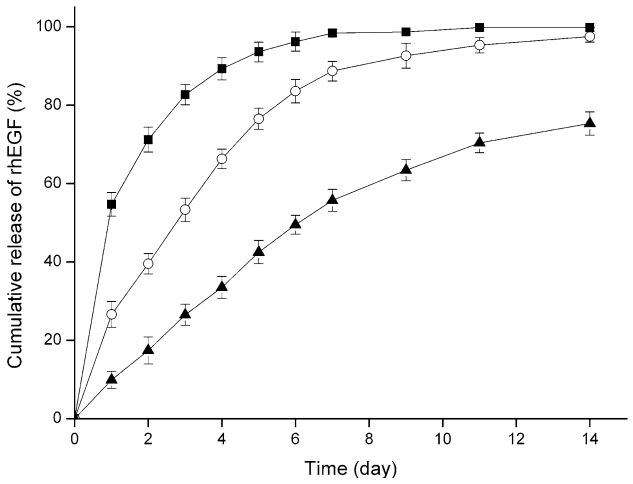

Fig. 6 Cumulative release of rhEGF from nanoparticle incorporated fibrin gels prepared at different fibrinogen concentrations [Table 2; Group V, fibrinogen, 25 mg/ml (*filled square*); Group II, fibrinogen, 50 mg/ml (*open circle*); Group VI, fibrinogen, 100 mg/ml (*filled triangle*)]. The values represent the mean ± S.D. ($n = 5$)

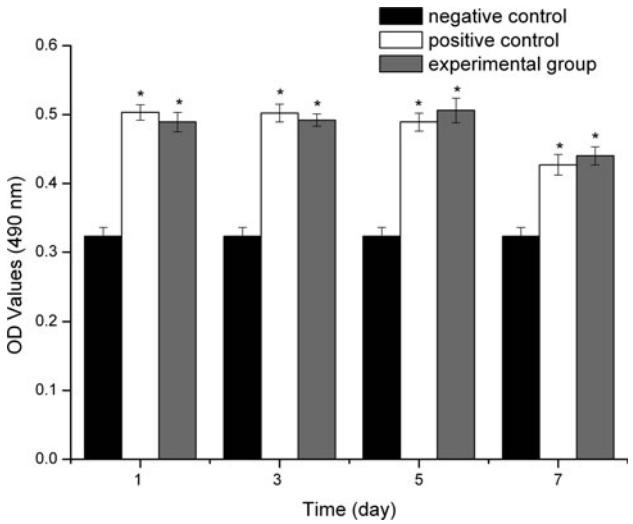

Fig. 7 MTT colorimetric assay of cell proliferation stimulated by rhEGF. Each value represents the mean ± SD of absorbance value (OD) for cells. Significant increases in optical density were seen in the experimental group and positive control compared with the negative control ($n = 7$, $^*P < 0.05$, Anova and post-hoc Bonferroni). There were no differences between experimental group and positive control

4 Discussion

Wound healing is quite a complicated process involving epidermal regeneration, fibroblast proliferation, neovascularization and synthesis [20]. Studies have shown that exogenous application of growth factors may decrease the healing period and improve the quality of wound healing [3, 21]. Growth factors bind to specific high-affinity receptors on the cell-surface to stimulate cell growth. Although they are present in small amounts, they exert a powerful influence on the process of wound repair. However, wound fluids have shown that the wound environment has the capacity to induce premature growth factor degradation and inactivation [22, 23]. Yang et al. [24] evaluated the stability of rhEGF in burn-injured pigs, and found that burn wound induced activity of acid proteolytic enzymes was the main explanation as the cause for rhEGF rapid degradation in the first day post-burn skin homogenate. In our study, rapid elimination of rhEGF was also observed in rabbit conjunctival homogenate (Fig. 2). Moreover, it was demonstrated that the first 5 days after injury were the most critical during which maximal differences were seen between rhEGF treated and untreated wounds. rhEGF application after this period produced no significant improvement over controls, since by this time reepithelialization had already occurred in both groups [25]. Therefore, developing a suitable delivery system for rhEGF is critical for the efficient application of rhEGF. The potential delivery system should (1) protect growth factors against enzymic hydrolysis when administrated in the wound site and (2) achieve a sustained and controlled release of growth factors. Trials have included liquids, gels, collagen sponges and nanoparticulate systems as delivery vehicles for the growth factor [26–29]. Although there have been some advances, the best treatment remains uncertain.

One of the promising approaches to develop an efficient delivery system for growth factors is to design a composite delivery system using two or more of the delivery vehicles mentioned above, which would combine their advantages and avoid their disadvantages. In the present work, we combined two widely used drug delivery vehicles, CS nanoparticles and fibrin glue, to develop a composite system for efficient delivery of rhEGF.

As for the first requirement, rhEGF-loaded CS nanoparticles were prepared and characterized. The stability of the rhEGF entrapped into nanoparticles was examined. In this study, CS naoparticles exhibited a relative high encapsulation efficiency (highest EE%: 67.03%, Table 1) compared with that reported in a previous study [30], in which bFGF-loaded CS nanoparticles were prepared using a same method and showed a relative low encapsulation efficiency (27.388%). The high EE% could be attributed to the negative charge of rhEGF (isoelectric point: 4.6), which may form an ionic crosslink with positively charged CS molecules. It was shown in this study that CS nanoparticles decreased the elimination of rhEGF in rabbit conjunctival homogenate, and thus show the advantage of protecting rhEGF from degradation (Fig. 2). Although many previous literatures have reported chitosan nanoparticles had the capacity to entrap a wide range of molecules and protect them from the harmful biological environment [31], little knowledge has been known about the mechanism of this

protective effect. Masuoka et al. [32] tested the interaction of chitosan with bFGF in their study, and found that soluble chitosan could protect the bFGF activity from inactivation, such as heat, proteolysis and acid. They gave an explanation that protective effect on bFGF by chitosan was due to the complex formation between the growth factor and chitosan through an interaction between the negatively-charged sites of the protein and positively-charged amino groups of the chitosan. During the rhEGF/CS nanoparticle preparation process in our study, rhEGF was first incorporated into the CS solution followed by stirring, which could lead to a similar ionic interaction between rhEGF and chitosan molecules. Based on the above, we presume that one of the ways in which the chitosan nanoparticles potentiated the rhEGF activity may be by protecting it from inactivation via the interaction between rhEGF and chitosan molecules. In addition, compared with CS solution, the nanoparticle formulation could form a physical block between the drug encapsulated and the harmful substances around, thus decrease the contact of rhEGF with proteolytic enzymes.

As for the second requirement, we examined the in vitro releases of rhEGF from nanoparticles, fibrin gel and the composite system: fibrin gel loaded with nanoparticles (Fig. 4). The release of rhEGF from CS nanoparticles sustained approximately for 72 h with an initial burst release. It has been known that protein release from chitosan particulate systems involves three different mechanisms [33]: (a) desorption of protein molecules from the surface of the particles, (b) diffusion through the swollen polysaccharide matrix and (c) release due to polymer erosion. The first mechanism plays the major role in the burst-release phase, and the slow-release phase is due to diffusion and polymer erosion. For fibrin gel, drugs are released in vitro by the simple diffusion through water phase, and the drawback of this system is the length of delivery does not make it applicable to long-term drug depot use [34]. It was observed that the release of rhEGF from the fibrin gel sustained approximately for 96 h. The nanoparticle-loaded fibrin gel offered a much more prolonged period of rhEGF release which sustained for about 14 days at the median concentrations of fibrinogen and thrombin (Fig. 5). So we believe that, after the incorporation of CS nanoparticles in the fibrin gel, the nanoparticle-loaded fibrin gel turns out to be a double diffusion-dependent drug release system. The release of rhEGF from this composite delivery system to the aqueous phase might involve three processes: rhEGF release from the gel, nanoparticle release from the gel, and rhEGF release from nanoparticles. Because rhEGF should travel through the two polymer matrices and the nanoparticles were released from the gel only slowly, the rhEGF release rate of the composite system was slower than for the others. However, it is relevant to underline that the growth factor release, obtained in this in vitro study, could be completed in vivo in a shorter time lapse because both CS and fibrin gel are biodegradable.

The advantages of fibrin gel as a drug delivery system have been well demonstrated in a recent review [34], one of which is that release kinetic can be tailored through composition, affinity and covalent linkage. As for the nanoparticle-loaded fibrin gel, we examined the effect of fibrinogen and thrombin concentrations on the rhEGF release kinetics, and found that the release rate of rhEGF from the composite gel can be controlled by adjusting the content of thrombin or fibrinogen (Fig. 5). This observation coincides with the previous findings [35]. As the concentration of fibrinogen or thrombin is increased in the composite gel, a densely crosslinked fibrin network is formed, and the release of rhEGF or nanoparticles from the fibrin network should be slowed. Compared with other gel system for drug delivery, another advantage of fibrin gel to be addressed is its biologic adhesiveness. This property makes it widely used in surgical and tissue engineering fields such as skin graft fixation, nerve repair, cartilage reattachment and microvascular anastomoses [36]. Eiichi Sekiyama et al. [37] used fibrin gel as a tissue adhesive and successfully performed a sutureless transplantation of amniotic membrane for ocular surface reconstruction. In those cases, the composite fibrin gel would be more useful for wound healing because, as a tissue adhesive, it would release growth factor in the meanwhile at wound site. However, it should be raised that we did not determine the adhesive property of the composite gel in this study. Though the microstructure of the composite gel seems not be changed (Fig. 3), further studies should be performed to investigate the effect of the incorporation of CS nanoparticles on its adhesive property.

At the end of the study, the in vitro proliferation of BALB/c 3T3 cells induced by rhEGF released from composite fibrin gels was evaluated to test their biological activity. It was found that the rhEGF preserved its bioactivity when compared to the negative control (in which no rhEGF were added to culture medium) and the positive control (in which rhEGF in free form were added to culture medium) at each time point (Fig. 7). Unlike some other formations of drug delivery system for growth factors, the whole preparation process of the composite gel did not involve the use of organic solvents and high temperatures, which would insure the bioactivity of rhEGF.

5 Conclusions

In this study, we successfully developed a novel delivery system for rhEGF: a fibrin gel loaded with chitosan

nanoparticles. Compared with other delivery systems for growth factors, it possesses the advantages of both chitosan nanoparticles and fibrin gel, including: (1) protection of growth factors from proteolysis; (2) sustained and controlled release for a much more prolonged period; (3) biologic adhesiveness; (4) biocompatible and injectable. The obtained composite fibrin gel may be useful for topical applications at the site of wounds such as ocular surface destructions, burns, fissures, ulcers, blisters, bone breaks etc., in which the release of growth factors are of critical importance in the promotion and speed of the healing process. In addition, it may have great potential application in tissue engineering.

Acknowledgments This work was supported by grants from the Chongqing Science and Technology Committee (CSTC, 2008AC0086) and the First Affiliated Hospital of Chongqing Medical University (YXJJ2009-09).

References

1. DiBiase MD, Rhodes CT. The design of analytical methods for use in topical epidermal growth factor product development. J Pharm Pharmacol. 1991;43(8):553–8.
2. Kitajima T, Sakuragi M, Hasuda H, Ozu T, Ito Y. A chimeric epidermal growth factor with fibrin affinity promotes repair of injured keratinocyte sheets. Acta Biomater. 2009;5(7):2623–32.
3. Grazul-Bilska AT, Johnson ML, Bilski JJ, Redmer DA, Reynolds LP, Abdullah A, et al. Wound healing: the role of growth factors. Drugs Today. 2003;39(10):787–800.
4. Mössner J, Caca K. Developments in the inhibition of gastric acid secretion. Eur J Clin Invest. 2005;35(8):469–75.
5. Trengove NJ, Stacey MC, MacAuley S, Bennett N, Gibson J, Burslem F, et al. Analysis of the acute and chronic wound environments: the role of proteases and their inhibitors. Wound Repair Regen. 1999;7(6):442–52.
6. Kim EY, Gao ZG, Park JS, Li H, Han K. rhEGF/HP-[beta]-CD complex in poloxamer gel for ophthalmic delivery. Int J Pharm. 2002;233(1–2):159–67.
7. Schneider A, Wang XY, Kaplan DL, Garlick JA, Egles C. Biofunctionalized electrospun silk mats as a topical bioactive dressing for accelerated wound healing. Acta Biomater. 2009;5(7):2570–8.
8. Agnihotri SA, Mallikarjuna NN, Aminabhavi TM. Recent advances on chitosan-based micro- and nanoparticles in drug delivery. J Control Release. 2004;100(1):5–28.
9. Mourya VK, Inamdar NN. Trimethyl chitosan and its applications in drug delivery. J Mater Sci Mater Med. 2009;20(5):1057–79.
10. Kumari A, Yadav SK, Yadav SC. Biodegradable polymeric nanoparticles based drug delivery systems. Colloids Surf B. 2010; 75(1):1–18.
11. Zhang XG, Teng DY, Wu ZM, Wang X, Wang Z, Yu DM, et al. PEG-grafted chitosan nanoparticles as an injectable carrier for sustained protein release. J Mater Sci Mater Med. 2008;19(12): 3525–33.
12. Hasanovic A, Zehl M, Reznicek G, Valenta C. Chitosan-tripolyphosphate nanoparticles as a possible skin drug delivery system for aciclovir with enhanced stability. J Pharm Pharmacol. 2009; 61(12):1609–16.
13. Sakiyama-Elbert SE, Hubbell JA. Controlled release of nerve growth factor from a heparin-containing fibrin-based cell in growth matrix. J Control Release. 2000;69(1):149–58.
14. Kaufman MR, Westreich R, Ammar SM, Amirali A, Iskander A, Lawson W. Autologous cartilage grafts enhanced by a novel transplant medium using fibrin sealant and fibroblast growth factor. Arch Facial Plast Surg. 2004;6(2):94–100.
15. Zisch AH, Schenk U, Schense JC, Sakiyama-Elbert SE, Hubbell JA. Covalently conjugated VEGF–fibrin matrices for endothelialization. J Control Release. 2001;72(1–3):101–13.
16. Giannoni P, Hunziker EB. Release kinetics of transforming growth factor-beta1 from fibrin clots. Biotechnol Bioeng. 2003; 83(1):121–3.
17. Gwak SJ, Kim SS, Sung K, Han J, Choi CY, Kim BS. Synergistic effect of keratinocyte transplantation and epidermal growth factor delivery on epidermal regeneration. Cell Transplant. 2005;14(10): 809–17.
18. Briganti E, Spiller D, Mirtelli C, Kull S, Counoupas C, Losi P, et al. A composite fibrin-based scaffold for controlled delivery of bioactive pro-angiogenetic growth factors. J Control Release. 2010;142(1):14–21.
19. Park JS, Yoon JI, Li H, Moon DC, Han K. Buccal mucosal ulcer healing effect of rhEGF/Eudispert hv hydrogel. Arch Pharm Res. 2003;26(8):659–65.
20. Alemdaroglu C, Degim Z, Celebi N, Zor F, Ozturk S, Erdogan D. An investigation on burn wound healing in rats with chitosan gel formulation containing epidermal growth factor. Burns. 2006; 32(3):319–27.
21. Werner S, Grose R. Regulation of wound healing by growth factors and cytokines. Physiol Rev. 2003;83(3):835.
22. Hardwicke J, Ferguson EL, Moseley R, Stephens P, Thomas DW, Duncan R. Dextrin-rhEGF conjugates as bioresponsive nanomedicines for wound repair. J Control Release. 2008;130(3):275–83.
23. Hardwicke J, Schmaljohann D, Boyce D, Thomas D. Epidermal growth factor therapy and wound healing–past, present and future perspectives. Surgeon. 2008;6(3):172–7.
24. Yang CH, Huang YB, Wu PC, Tsai YH. The evaluation of stability of recombinant human epidermal growth factor in burn-injured pigs. Process Biochem. 2005;40(5):1661–5.
25. Buckley A, Davidson JM, Kamerath CD, Woodward SC. Epidermal growth factor increases granulation tissue formation dose dependently. J Surg Res. 1987;43(4):322–8.
26. Hori K, Sotozono C, Hamuro J, Yamasaki K, Kimura Y, Ozeki M, et al. Controlled-release of epidermal growth factor from cationized gelatin hydrogel enhances corneal epithelial wound healing. J Control Release. 2007;118(2):169–76.
27. Yang CH. Evaluation of the release rate of bioactive recombinant human epidermal growth factor from crosslinking collagen sponges. J Mater Sci Mater Med. 2008;19(3):1433–40.
28. Zhang S, Uludag H. Nanoparticulate systems for growth factor delivery. Pharm Res. 2009;26(7):1561–80.
29. Schultz CL, Morck DW. Contact lenses as a drug delivery device for epidermal growth factor in the treatment of ocular wounds. Clin Exp Optom. 2010;93(2):61–5.
30. Cetin M, Aktas Y, Vural I, Capan Y, Dogan LA, Duman M, et al. Preparation and in vitro evaluation of bFGF-loaded chitosan nanoparticles. Drug Deliv. 2007;14(8):525–9.
31. Amidi M, Mastrobattista E, Jiskoot W, Hennink WE. Chitosan-based delivery systems for protein therapeutics and antigens. Adv Drug Deliv Rev. 2010;62(1):59–82.
32. Masuoka K, Ishihara M, Asazuma T, Hattori H, Matsui T, Takase B, et al. The interaction of chitosan with fibroblast growth factor-2 and its protection from inactivation. Biomaterials. 2005;26(16): 3277–84.
33. Zhou S, Deng X, Li X. Investigation on a novel core-coated microspheres protein delivery system. J Control Release. 2001;75(1–2):27–36.
34. Spicer PP, Mikos AG. Fibrin glue as a drug delivery system. J Control Release. 2010;148(1):49–55.

35. Jeon O, Ryu SH, Chung JH, Kim BS. Control of basic fibroblast growth factor release from fibrin gel with heparin and concentrations of fibrinogen and thrombin. J Control Release. 2005; 105(3):249–59.
36. Lee SB, Geroski DH, Prausnitz MR, Edelhauser HF. Drug delivery through the sclera: effects of thickness, hydration, and sustained release systems. Exp Eye Res. 2004;78(3):599–607.
37. Sekiyama E, Nakamura T, Kurihara E, Cooper LJ, Fullwood NJ, Takaoka M, et al. Novel sutureless transplantation of bioadhesive-coated, freeze-dried amniotic membrane for ocular surface reconstruction. Invest Ophthalmol Vis Sci. 2007;48(4):1528–34.